

## Multiple Pounding Tuned Mass Damper (MPTMD) control on benchmark tower subjected to earthquake excitations

Wei Lin<sup>\*1</sup>, Yinglu Lin<sup>1a</sup>, Gangbing Song<sup>2b</sup> and Jun Li<sup>3c</sup>

<sup>1</sup>*School of Civil Engineering, Fuzhou University, China*

<sup>2</sup>*Department of Mechanical Engineering, University of Houston, USA*

<sup>3</sup>*Centre for Infrastructural Monitoring and Protection, School of Civil and Mechanical Engineering, Curtin University, Kent Street, Bentley, WA 6102, Australia*

*(Received March 30, 2016, Revised May 23, 2016, Accepted June 26, 2016)*

**Abstract.** To explore the application of traditional tuned mass dampers (TMDs) to the earthquake induced vibration control problem, a pounding tuned mass damper (PTMD) is proposed by adding a viscoelastic limitation to the traditional TMD. In the proposed PTMD, the vibration energy can be further dissipated through the impact between the attached mass and the viscoelastic layer. More energy dissipation modes can guarantee better control effectiveness under a suite of excitations. To further reduce mass ratio and enhance the implementation of the PTMD control, multiple PTMDs (MPTMD) control is then presented. After the experimental validation of the proposed improved Hertz based pounding model, the basic equations of the MPTMD controlled system are obtained. Numerical simulation is conducted on the benchmark model of the Canton Tower. The control effectiveness of the PTMD and the MPTMD is analyzed and compared under different earthquake inputs. The sensitivity and the optimization of the design parameters are also investigated. It is demonstrated that PTMDs have better control efficiency over the traditional TMDs, especially under more severe excitation. The control performance can be further improved with MPTMD control. The robustness can be enhanced while the attached mass for each PTMD can be greatly reduced. It is also demonstrated through the simulation that a non-uniformly distributed MPTMD has better control performance than the uniformly distributed one. Parameter study is carried out for both the PTMD and the MPTMD systems. Finally, the optimization of the design parameters, including mass ratio, initial gap value, and number of PTMD in the MPTMD system, is performed for control improvement.

**Keywords:** pounding tuned mass damper (PTMD); pounding force model; vibration control; benchmark tower; earthquake excitation

### 1. Introduction

Nowadays, higher and more complex civil structures have being constructed all around the world. Earthquake has always been a major hazard that endangers the safety of structures. To fully

---

\*Corresponding author, Associate Professor, E-mail: [cewlin@fzu.edu.cn](mailto:cewlin@fzu.edu.cn)

<sup>a</sup>Master student, E-mail: [595077538@qq.com](mailto:595077538@qq.com)

<sup>b</sup>Professor, E-mail: [gsong@uh.edu](mailto:gsong@uh.edu)

<sup>c</sup>Senior lecturer, E-mail: [junli@curtin.edu.au](mailto:junli@curtin.edu.au)

predict the excitations exerted on the structures during their service stage is nearly impossible. Also, the cost of the construction may be greatly increased if more possible loadings and vibrations are taken into account in the design. Structural control is believed to be an effective approach to enhance the adaptability of the structures and their safety during earthquakes (Emiliano 2015, Li *et al.* 2015, Maki 2015, Takewaki 2013). Tuned mass dampers (TMDs) are one type of the earliest passive control devices, and have been regarded as an effective measure against vibrations induced by wind loads and some harmonic loadings, e.g., pedestrian excitations (Soong and Spencer 2002, Mishra *et al.* 2013, Zhen *et al.* 2013). Thus, TMDs have been applied to many high-rise buildings and footbridges to suppress undesirable vibrations, for example the Taipei 101 building and the London Millennium Bridge (Lee *et al.* 2006). A TMD absorbs inertial force from the main structure to reduce its motion. The control effectiveness is mainly determined by the dynamic characteristics, stroke and the amount of added mass of the TMD. With the development and control potential of TMDs, they have been applied to solve the vibration control problem induced by more complicated excitations, such as earthquakes.

However, studies have shown that TMDs can only reduce vibration components with frequencies close to the tuned frequencies. In operation, a TMD is often tuned to the natural frequency of the main structure or the dominant frequency of the excitation. Hence, the TMD has the most significant limitation of narrow effective bandwidth and high sensitivity to the frequency tuning (Nagarajaiah 2009, Casado *et al.* 2007, Occhiuzzi *et al.* 2008, Weber and Feltrin 2010), which makes it unsuitable for vibration control under broadband earthquake inputs (Hoang *et al.* 2008). As a result, various schemes have been proposed to improve the TMD for better robustness and reliability. Among which, the control approach with multiple TMDs (MTMD) has been developed by installing multiple TMDs on a structure with each tuned to different target frequency. The resulting control system is able to cover wider bandwidth with reduced weight of each TMD. The MTMD was used to control the buffeting problem of the Yangpu Bridge (Gu *et al.* 2001). Li and Ni (2007) analyzed a non-uniformly distributed MTMD system to demonstrate that it has better control performance over the traditional uniformly distributed MTMD (Yael 2015). However, many problems arise when applying the MTMD to earthquake induced vibration control. Mohtasham *et al.* (2013) used genetic algorithm to study the optimal parameter of MTMD, including the mass ratio, the number of TMDs and external excitation. Compared with other parameters, TMD's number was found to be less influential. Some researchers tried to figure out optimal location of TMDs under wind excitation. Multi-mode control scheme were adopted and each TMD was tuned in accordance with corresponding vibration mode. The results have shown impressive improvement against wind induced vibration (Shan Lang lu 2014 and Said Elias 2014). Richard *et al.* (2015) tried to take both locations and parameters of MTMD into account. Numerical analysis was conducted on different buildings. With the increase of mass ratio, the optimal location is going down. The control effectiveness of MTMD systems under seismic excitation was also validated. However, the complicated coupling effect between different TMDs makes it difficult to design an optimal parameter sets in certain control cases. It is also indicated that the control effectiveness of the MTMD system varies greatly with the frequency component of excitations, and is still very sensitive to the shifted natural frequencies of the main structure.

Some researchers tried to combine active or semi-active control devices with TMDs. For example, TMDs combined with nonlinear hysteretic damper turn out to have better control efficiency (Rüdinger 2006 and 2007, Alexander and Schilder 2009, Chung *et al.* 2009); Active mass dampers (AMD) have been developed and widely used in the civil engineering field (Ikeda *et al.* 2001, Li *et al.* 2011). Some smart material and semi-active control approaches are also

incorporated with TMDs, hybrid controls like TMD-MR, TMD-SMA controls (Sun and Li 2009, Mishra *et al.* 2013, Weber and Maślanka 2012, Eason *et al.* 2013) are presented and proved to have better control performance and robustness.

Although TMDs incorporated with smart control devices can produce better control effectiveness and robustness to some extent, the two control elements works independently in most combined systems. In other words, the improvement of control is resulted from the inherit merits of the incorporated smart control devices rather than the working of TMDs. Besides, some combined control systems can only function normally with instant feedback. Usually, many sensors are required for reliable feedback, which increases the cost of the control system. Moreover, the incorporated control system may not be guaranteed to function normally under severe events. This paper seeks possible energy dissipation pattern for TMDs. By adding a limitation attached with viscoelastic layer to traditional TMDs, pounding tuned mass damper (PTMD) is adopted for the earthquake mitigation problems of high-rise structures. In a PTMD, a large amount of vibration energy can be dissipated through the impact behavior between the mass and the limitation. The nonlinear deformation of the viscoelastic layer will also dissipate the vibration energy of the host structure into heat energy. The control efficiency of the PTMD and the superiority over TMD are to be verified through a comprehensive numerical study on an earthquake excited super tall benchmark TV tower. Both single PTMD control and multiple PTMD (MPTMD) control are considered and detailed parameter study is presented.

## 2. Schematic model Pounding Tuned Mass Damper (PTMD)

An application of single PTMD on the vibration control problem of high-rise structure under wind load and earthquake excitations is proposed. The research work detailed the design of a PTMD according to the dynamic characteristic of the host structure.

As shown in Fig. 1, a PTMD consists of a TMD and a viscoelastic limitation. When there is only slight oscillation of the mass, the damper acts as a TMD, which can dissipate vibration energy through the movement of the attached mass. When the oscillation is large enough to generate an impact between the mass and the viscoelastic layer, the device acts like a pounding damper, by which energy can be dissipated through the impact behavior. Moreover, the deformation of the viscoelastic material during an impact can further transfer some vibration energy into heat energy. During operation, a PTMD can somehow switch its energy dissipation modes in between a TMD and a pounding damper. It is worth mentioning that unlike semi-active or active devices, after

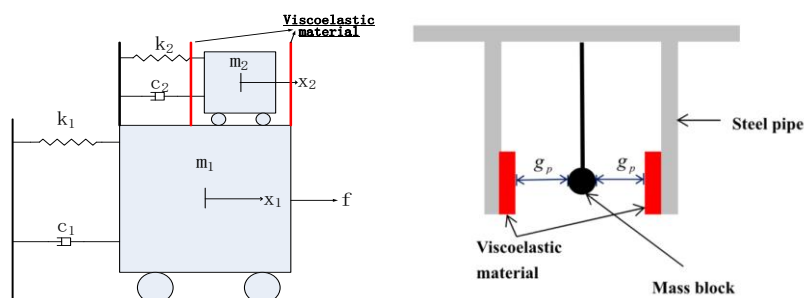


Fig. 1 Schematic model and prototype of PTMD

prescribing a set of parameters, a PTMD is expected to switch automatically according to the severity and frequency components of the vibration. The switching mechanism enables the PTMD to effectively reduce the vibration of the structure under excitations with more bandwidth.

### 3. Modeling of MPTMD controlled system

The equations of motion of a free structure under earthquake excitation has the form of

$$\mathbf{M}_s \ddot{\mathbf{X}}_s + \mathbf{C}_s \dot{\mathbf{X}}_s + \mathbf{K}_s \mathbf{X}_s = -\mathbf{M}_s \ddot{\mathbf{x}}_g \quad (1)$$

in which  $\mathbf{M}_s$ ,  $\mathbf{C}_s$ ,  $\mathbf{K}_s$  are  $n \times n$  mass, damping and stiffness matrixes of the structure; subscription  $s$  stands for structure;  $\ddot{\mathbf{x}}_g$  is the earthquake acceleration. Assuming the  $(n-r)$ <sup>th</sup> to  $n$ <sup>th</sup> DOFs are attached with  $r$  PTMDs, the controlled system coupled with multiple PTMDs are expressed as

$$\begin{bmatrix} \mathbf{M}_s & \mathbf{O} \\ \mathbf{O} & \mathbf{M}_r \end{bmatrix} \begin{bmatrix} \ddot{\mathbf{X}}_s \\ \ddot{\mathbf{X}}_r \end{bmatrix} + \begin{bmatrix} \mathbf{C}_{ss} & \mathbf{C}_{sr} \\ \mathbf{C}_{rs} & \mathbf{C}_{rr} \end{bmatrix} \begin{bmatrix} \dot{\mathbf{X}}_s \\ \dot{\mathbf{X}}_r \end{bmatrix} + \begin{bmatrix} \mathbf{K}_{ss} & \mathbf{K}_{sr} \\ \mathbf{K}_{rs} & \mathbf{K}_{rr} \end{bmatrix} \begin{bmatrix} \mathbf{X}_s \\ \mathbf{X}_r \end{bmatrix} = - \begin{bmatrix} \mathbf{M}_s & \mathbf{O} \\ \mathbf{O} & \mathbf{M}_r \end{bmatrix} \ddot{\mathbf{x}}_g - \begin{bmatrix} \mathbf{D}_s & \mathbf{O} \\ \mathbf{O} & \mathbf{D}_r \end{bmatrix} \begin{bmatrix} \mathbf{P}_s \\ \mathbf{P}_r \end{bmatrix} \quad (2)$$

where subscription  $r$  indicates the DOFs corresponding to the PTMD mass;  $\mathbf{C}_r$  and  $\mathbf{K}_r$  are formed according to the connecting damping and stiffness of each PTMD;  $\mathbf{D}$  is the index matrix indicating the DOFs of the control forces;  $\mathbf{P}$  is the pounding force value between the attached mass and the viscoelastic layer, named  $P_s$  and  $P_r$  for the structure and the PTMDs, respectively; and  $\mathbf{C}_{sr}$ ,  $\mathbf{C}_{ss}$ ,  $\mathbf{K}_{ss}$  and  $\mathbf{K}_{sr}$  are written as

$$\begin{aligned} \mathbf{C}_{ss} = \mathbf{C}_s + \bar{\mathbf{C}}_s = \mathbf{C}_s + \begin{bmatrix} \mathbf{O} & \mathbf{O} \\ c_1 & 0 & 0 \\ \mathbf{O} & 0 & \mathbf{O} & 0 \\ 0 & 0 & 0 & c_r \end{bmatrix} \quad \mathbf{K}_{ss} = \mathbf{K}_s + \bar{\mathbf{K}}_s = \mathbf{K}_s + \begin{bmatrix} \mathbf{O} & \mathbf{O} \\ k_1 & 0 & 0 \\ \mathbf{O} & 0 & \mathbf{O} & 0 \\ 0 & 0 & 0 & k_r \end{bmatrix} \\ \mathbf{C}_{sr} = \mathbf{C}_{rs}^T = \begin{bmatrix} -c_{r1} & 0 & 0 & 0 \\ 0 & -c_{r2} & 0 & 0 \\ \mathbf{M} & \mathbf{M} & \mathbf{O} & \mathbf{M} \\ 0 & 0 & 0 & -c_{rn} \end{bmatrix} \quad \mathbf{K}_{sr} = \mathbf{K}_{rs}^T = \begin{bmatrix} -k_{r1} & 0 & 0 & 0 \\ 0 & -k_{r2} & 0 & 0 \\ \mathbf{M} & \mathbf{M} & \mathbf{O} & \mathbf{M} \\ 0 & 0 & 0 & -k_{rn} \end{bmatrix} \end{aligned} \quad (3)$$

For a single PTMD, the equations of motion of the  $r$ <sup>th</sup> PTMD can be extracted from Eq. (2) as

$$m_r \ddot{x}_r - c_r \dot{x}_n + c_r \dot{x}_r - k_r x_n + k_r x_r = -p \quad (4)$$

Eq. (4) can be rewritten as

$$m_r \ddot{x}_r + c_r \dot{x}_r + k_r x_r = k_r x_n + c_r \dot{x}_n - p \quad (5)$$

The terms  $k_r x_n + c_r \dot{x}_n$  in Eq. (5) can be considered as the external force applied to the PTMD mass. Further extracting the equations of motion of the structure yields

$$\mathbf{M}_s \ddot{\mathbf{X}}_s + \mathbf{C}_s \dot{\mathbf{X}}_s + \mathbf{K}_s \mathbf{X}_s = -\mathbf{M}_s \ddot{\mathbf{x}}_g - \mathbf{M}_r \ddot{\mathbf{X}}_r - \begin{bmatrix} \bar{\mathbf{C}}_s & \mathbf{C}_{sr} \end{bmatrix} \begin{bmatrix} \dot{\mathbf{X}}_s \\ \dot{\mathbf{X}}_r \end{bmatrix} - \begin{bmatrix} \mathbf{K}_s & \mathbf{K}_{sr} \end{bmatrix} \begin{bmatrix} \mathbf{X}_s \\ \mathbf{X}_r \end{bmatrix} - \mathbf{D}_s \mathbf{P}_s \quad (6)$$

It is clear from Eq. (6) that the control force produced by a MPTMD system contains several

components, as the energy can be dissipated through kinetic energy, internal energy, potential energy, as well as pounding energy.

#### 4. Improved pounding force model and experimental validation

The impact between rigid bodies can be described by many models, but the precision is questionable when viscoelastic material is included. As one of the popular numerical models, the contact model based on the Hertz contact theory was first adopted to predict the pounding force of PTMDs in the previous study. As shown in Fig. 2, a small-scale experiment was set up to verify the numerical model. A motor is used in the experiment to generate impact between a mass and a limitation attached with several layers of viscoelastic material. The viscoelastic material is selected as 3M VHB4936 in the experiments. Keyence Lb11 laser sensor is used to capture the displacement of the mass. Both sinusoidal and random signals are generated to excite the motor. The data is collected by dSPACE 1104 with the sampling frequency being set as 1000 Hz.

Hertz based numerical model (Flores *et al.* 2011) is expressed as

$$P(t) = \begin{cases} \beta [u_1(t) - u_2(t) - g_p]^{3/2} + c [\dot{u}_1(t) - \dot{u}_2(t)] & u_1(t) - u_2(t) - g_p > 0 \text{ and } \dot{u}_1(t) - \dot{u}_2(t) > 0 \\ \beta [u_1(t) - u_2(t) - g_p]^{3/2} & u_1(t) - u_2(t) - g_p > 0 \text{ and } \dot{u}_1(t) - \dot{u}_2(t) < 0 \\ 0 & u_1(t) - u_2(t) - g_p < 0 \end{cases} \quad (7)$$

where  $u_1$  and  $u_2$  are the absolute displacements of the mass and the limitation, and  $g_p$  is the initial gap value, which refers to the preset gap value between the mass and the limitation.  $\beta$  is the pounding stiffness coefficient that mainly depends on the material properties and the geometry of colliding bodies.  $c$  is the impact damping, which at any instant of time can be obtained by

$$c = 2\xi \sqrt{\beta \sqrt{u_1 - u_2 - g_p} \frac{m_1 m_2}{m_1 + m_2}} \quad (8)$$

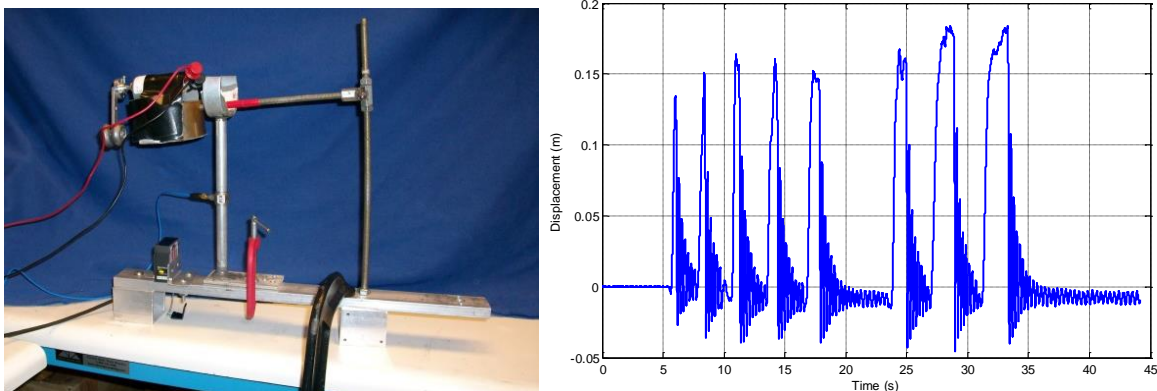


Fig. 2 Experimental setup and recorded displacement

$$\xi = \frac{9\sqrt{5}}{2} \frac{1-e^2}{e(e(9\pi-16)+16)} \tag{9}$$

where  $m_1$  and  $m_2$  are the masses of the two colliding bodies, and  $\xi$  is the impact damping ratio correlated with the coefficient of restitution  $e$ , which can be determined by calculating the ratio of the rebound height  $h^f$  and the original height  $h^0$

$$e = \sqrt{h^f/h^0} \tag{10}$$

In the case of fully elastic impact case,  $h^f=h^0$ ; while in the case of perfectly plastic impact,  $e=0$ .

The parameters are updated based on the captured signal. Through the comparison of the predicted and the experimental results, it is found that the traditional Hertz based model tends to underestimate the peak pounding force. By taking into account the nonlinear deformation of the viscoelastic layer during collision, an improved nonlinear impact damping is proposed for compensation of the traditional Hertz based impact model. The compensation of the nonlinear damping is assumed to be sensitive to the relative velocity between the two collision bodies. The improved Hertz based model and the nonlinear impact damping is expressed as

$$P(t) = \begin{cases} \bar{\beta} [u_1(t) - u_2(t) - g_p]^{s_1} + \bar{c}(t) [\dot{u}_1(t) - \dot{u}_2(t)] & u_1(t) - u_2(t) - g_p > 0 \text{ and } \dot{u}_1(t) - \dot{u}_2(t) > 0 \\ \bar{\beta} [u_1(t) - u_2(t) - g_p]^{s_1} & u_1(t) - u_2(t) - g_p > 0 \text{ and } \dot{u}_1(t) - \dot{u}_2(t) < 0 \\ 0 & u_1(t) - u_2(t) - g_p < 0 \end{cases} \tag{11}$$

$$\bar{c}(t) = 2\bar{\xi}_1 \sqrt{\bar{\beta} \sqrt{\delta(t)} \frac{m_1 m_2}{m_1 + m_2}} + \bar{\xi}_2 \dot{\delta}(t)^{s_2} \tag{12}$$

Table 1 Optimized parameters of modified pounding model

Parameters	$\beta_1$	$\xi_2$	$s_1$	$s_2$
value	10560	0.8	1.3	1.1

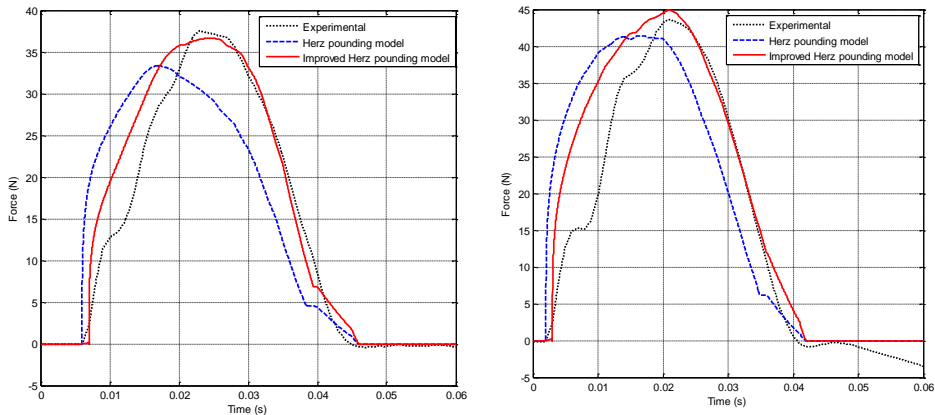


Fig. 3 Comparison of the improved and traditional pounding force model

in which  $\xi_1$  is the damping ratio correlated with the coefficient of restitution  $e$  given in Eq. (10), and  $\xi_2$  is the damping ratio correlated with the approaching velocity.  $\beta, \xi_2, s_1, s_2$  are relevant to the characteristics of the viscoelastic material parameters and need to be decided for this model. According to the experimental results, the identified parameters are listed in Table 1. Fig. 3 illustrates the comparison of experimental results and the predicted pounding force using both the improved Hertz model and traditional Hertz model.

## 5. Design of the PTMD and MPTMD

### 5.1 PTMD design

In a single PTMD case, a PTMD is first designed as a traditional TMD. Then the characteristic of the viscoelastic limitation is determined. For high-rise buildings, the top of the building is usually an optimal position to install a TMD. The control effectiveness of a TMD is better with larger mass ratio. Here mass ratio is the ratio of the added mass and the first order modal mass of the host structure. However, considering the bearing capacity of the host structure and the installation difficulty, the mass ratio is usually selected between 2‰ to 5‰. The stiffness and optimal damping ratio of the connection can be calculated by

$$k = m_0(2\pi f_1)^2 \quad (13)$$

$$\zeta_{opt} = \sqrt{\frac{3\mu_t}{8 \cdot (1 + \mu_t)}} \quad (14)$$

where  $f_1$  is the desired frequency to be tuned, and is decided according to the first natural frequency of the structure or the dominant excitation frequency of the excitation;  $m_0$  is the weight of the TMD mass installed on the structure; and  $\mu_t = m_0 / m_1$  denotes the ratio of the TMD mass to the generalized mass of the tuned mode.

The characteristic of the limitation is designed next. After carefully chosen the viscoelastic material and the thickness of the layer, parameters  $\beta, \xi_2, s_1, s_2$  in Eq. (11) are determined. The initial gap value plays an important role in maintaining the control performance and robustness of the PTMD. On one hand, too large gap value will lead to fewer collision times and smaller relative velocity between the two collision objects before the impact. In that case, a PTMD acts as a traditional TMD, and little energy can be dissipated through the impact behavior. On the other hand, smaller gap value cannot guarantee more pounding energy either. If too small a gap value is, the oscillation of the mass will be limited to a certain range and less kinetic energy can be transferred. As a result, an appropriate gap value should be carefully chosen according to the vibration amplitude of the mass in TMD cases. Besides, the optimal gap value may be affected by the intensity of the excitation. In the following parameter study, the variation of the control effectiveness with different initial gap values will be discussed in detail.

### 5.2 MPTMD design

Frequency characteristics is the most important issue for an MPTMD system. One solution is to design the MPTMD system based on the theory of MTMD system (Gu *et al.* 2001). Assuming the

mass of each PTMD is the same, and  $r$  PTMDs are installed and tuned to  $f_1, f_2, \dots, f_r$ , respectively.  $f_1$  and  $f_r$  refer to the lowest and highest frequencies in the MPTMD system,  $f_s$  is the first natural frequency of the host structure. The frequencies of other TMDs increase at an equal frequency increment towards both ends of the MPTMD system. Taking  $f_m$  the central frequency, the central frequency ratio  $\gamma_{cf}$  and the frequency-bandwidth ratio  $\gamma_{fw}$  are defined as

$$\gamma_{cf} = \frac{f_m}{f_s}, f_m = \frac{1}{r} \sum_{i=1}^r f_i \quad (14)$$

$$\gamma_{fw} = \frac{|f_k - f_1|}{f_s} \quad (15)$$

These two parameters completely describe the frequency characteristics of the MPTMD. The reduction ratio of the PTMD system will vary with different selection of these parameters.

In the above approach, the design of the MPTMD is based on certain constrains of uniformly distributed masses and frequencies. Unlike MTMD, MPTMD with more effective pounding and more serious deformation of viscoelastic layer can dissipate extra vibration energy. Hence, another approach to design the frequency characteristic is to use non-uniformly distributed frequencies, or non-uniformly distributed masses and initial gap value for each PTMD. In the following study, only the non-uniformly distributed frequencies are considered. In this case, the tuned frequencies are consistent with the first few natural frequencies of the structure. The position of each PTMD is decided based on the mode shapes corresponding to the tuned frequency.

## 6. Numerical simulations

### 6.1 Benchmark model

In numerical simulation, a benchmark model of a high-rise TV tower, the Canton tower located in Guangzhou, China, is selected as the structure. It is composed of the steel outer tube and a concrete inner tube. The total height of the structure is 600 m with a 146 m high antenna. A comprehensive structural health monitoring (SHM) system has been installed and has continuously recorded the structural information such as acceleration, stain, as well as earthquake and wind load excitation data. In order to set up a platform for the SHM research of super-tall building, a benchmark model is established (Ni *et al.* 2012). Both the full-order finite element (FE) and the reduced-order model are validated by the real measurement data. The reduced-order model is adopted in this study. The model contains of 37 beam elements and 38 nodes. Each node is assumed to have 5 DOFs, including two horizontal translational and three rotational DOFs. The damping ratio is 0.04 in this study. Fig. 4 shows the benchmark model with its first ten natural frequencies listed in Table 2. Hereafter, the directions  $x$  and  $y$  represent the direction along the long-axis and the short-axis of the bottom section.

Table 2 natural frequencies of the reduced-order model

Mode	1	2	3	4	5
Frequency (Hz)	0.110	0.159	0.347	0.368	0.399
Mode	6	7	8	9	10
Frequency (Hz)	0.460	0.485	0.738	0.902	0.997

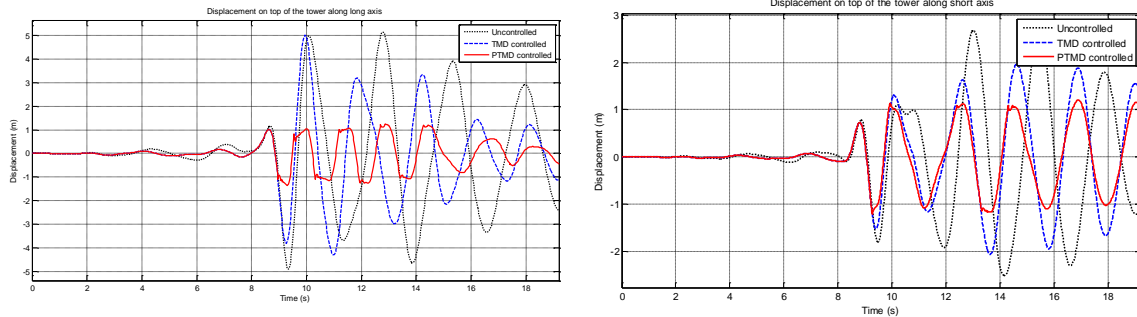


Figure 4 Benchmark model of Canton Tower

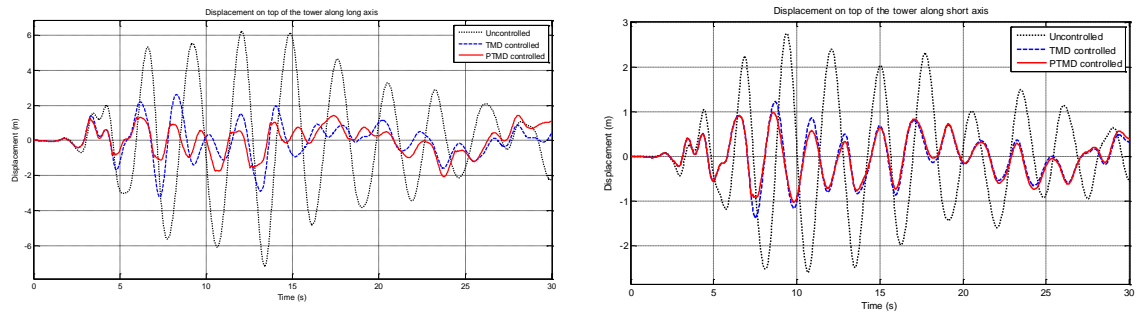
To verify the control effectiveness of the PTMD, Tianjin earthquake record and El Centro earthquake record are used to excite the structure and the controlled system. Earthquake components along  $x$ - and  $y$ - directions are considered simultaneously with the ratio of peak accelerations of 1:0.85. The intensities of the earthquakes are taken as 0.1 g to 0.3 g to generate different impact severity. Both the displacement and acceleration responses on the tower top are compared. In every case, the reduction rate of peak response to root-mean-square (RMS) response is examined.

### 6.2 Application of single PTMD control

For comparison with the control result of MPTMD cases, some of the results from the previous paper are briefly repeated here. Fig. 5 shows the comparison of uncontrolled, TMD controlled and PTMD controlled time-history displacement responses on the tower top, when the attached mass is fixed as 300 t and the initial gap value is set as 0.25 m. It is clear from the figures that the TMD control has limit reduction ratio, and also the reduction ratio is very sensitive to the inputs. On the contrary, PTMD controls can effectively reduce earthquake induced vibration, more than 60% of the reduction ratio of the peak and RMS responses can be expected.



(a) Tianjin earthquake record, 0.3 g

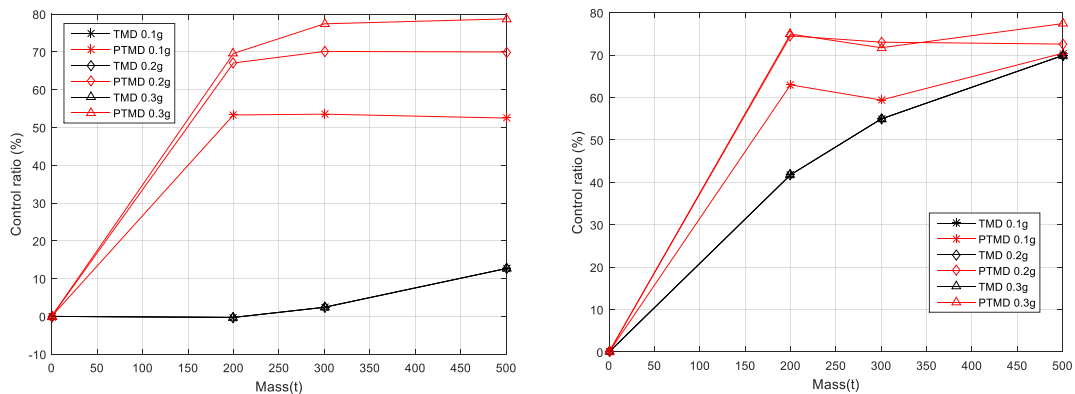


(b) El Centro earthquake record, 0.3 g

Fig. 5 Comparison of displacement responses and pounding force on the tower top

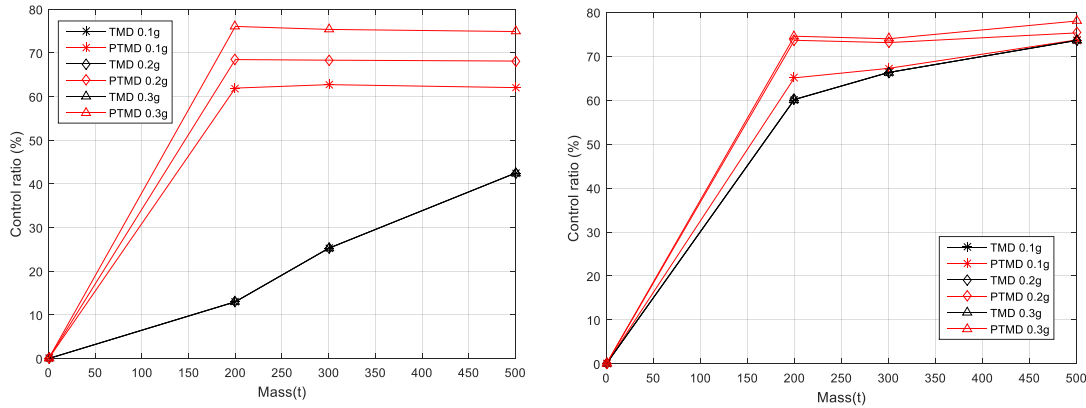
6.3 Influence of mass ratio and initial gap value

In Fig. 6, the control effectiveness of TMD and PTMD controls is analyzed with the variation of mass ratio. The attached mass of the TMD and the PTMD is selected as 200 t, 300 t and 500 t. The results indicates that the mass ratio seems to have large influence on the control effectiveness



(a) Control effectiveness of peak responses under Tianjin and El Centro excitations

Fig. 6 Variation of control effectiveness with mass ratio



(b) Control effectiveness of RMS responses under Tianjin and El Centro excitations  
Fig. 6 Continued

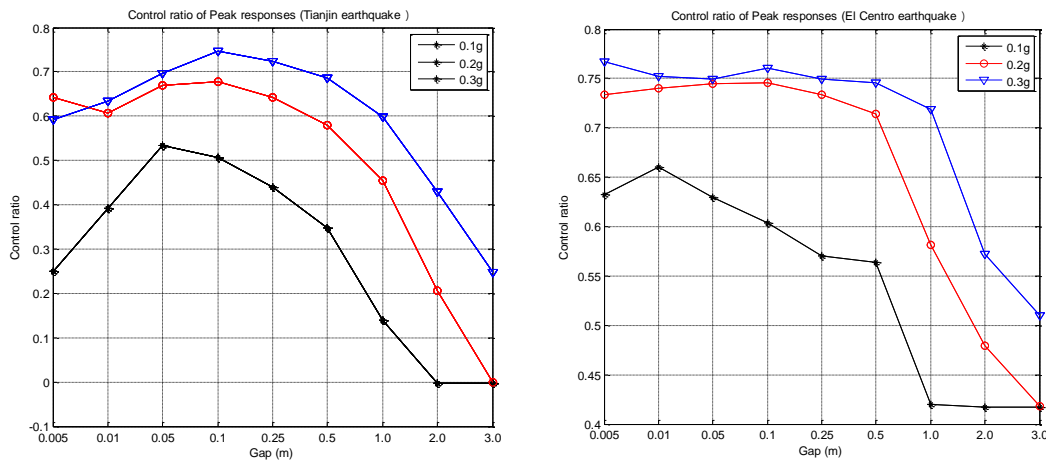


Fig. 7 Control effectiveness with different gap value (Mass: 200 t)

of the TMD controls. As for the PTMD controls, the fluctuation of the control ratio is small with the increasing mass ratio. Another issue can be also concluded from the figure that PTMDs are expected to have better performances under more severe excitations. For instance, more than 70% reduction is observed under earthquake strikes with the peak acceleration of 0.3 g. The reason is that higher intensity of the excitations tends to generate more frequent impact and more pounding energy during each impact.

Fig. 7 shows the influence of the initial gap value in the range between 0.005 m and 3 m. As shown in the figure, too large or too small of a gap value may harm the control effectiveness of the PTMD. A PTMD will perform as a traditional TMD when the gap reaches a certain value. It is also noticed that there must be an optimal solution for the best control ratio, but the optimal value may vary with the excitations.

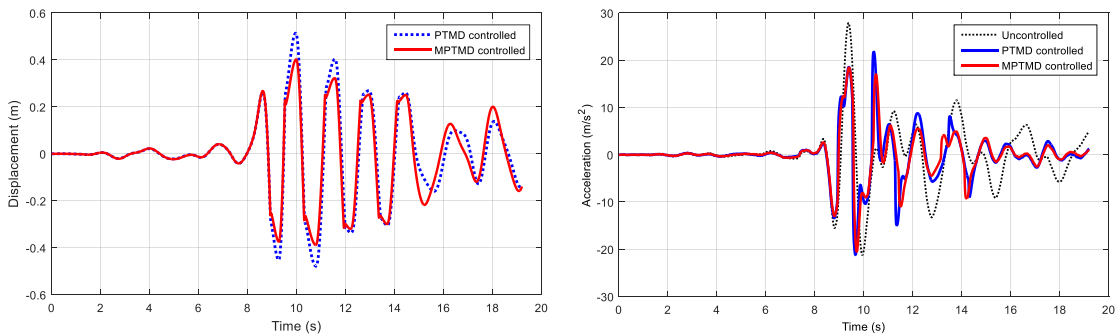
6.4 Vibration control with multiple PTMD (MPTMD)

To further reduce mass ratio and enhance the implementation of the PTMD control, multiple PTMD control cases are investigated. Instead of only using a single PTMD, multiple PTMDs are installed in different levels and the total mass is set to be equal to the single PTMD case to guarantee a comparative result. Furthermore, it is also expected that multiple PTMDs can cover wider frequency bands and produce better control results.

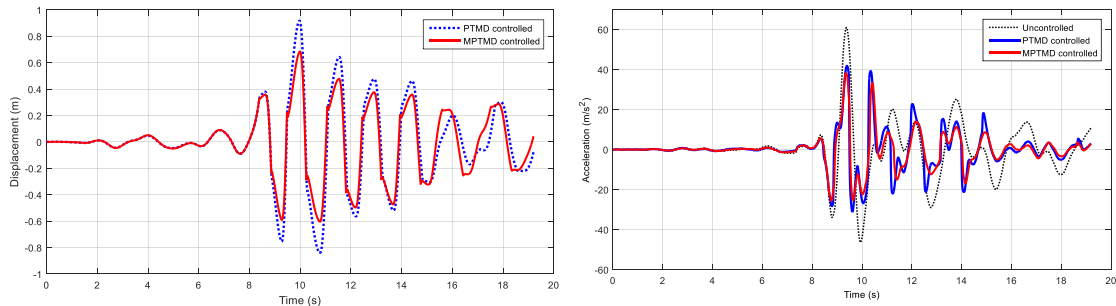
In the following cases, the aforementioned Tianjin earthquake record are adopted to excite the structure. Firstly, three PTMDs are considered to be attached to the top 3 nodes of the main tower, with each weighting 105 t. The frequencies of the PTMDs are tuned as the same as the first three natural frequencies of the TV Tower, respectively. The gap value of each PTMD is carefully chosen after several trail calculation. The detailed parameters of MPTMD are listed in Table 3. For

Table 3 Parameters of MPTMD

PTMD Number	Mass ratio $\mu$	mass(t)	Spring stiffness ( $N \cdot m^{-1}$ )	Pounding stiffness ( $N / m^{3/2}$ )	Frequency	$g_p$ (m)
1	0.5%	105	50106	17259	0.110	0.25
2	0.5%	105	104690	17259	0.159	0.25
3	0.5%	105	498620	17259	0.347	0.25

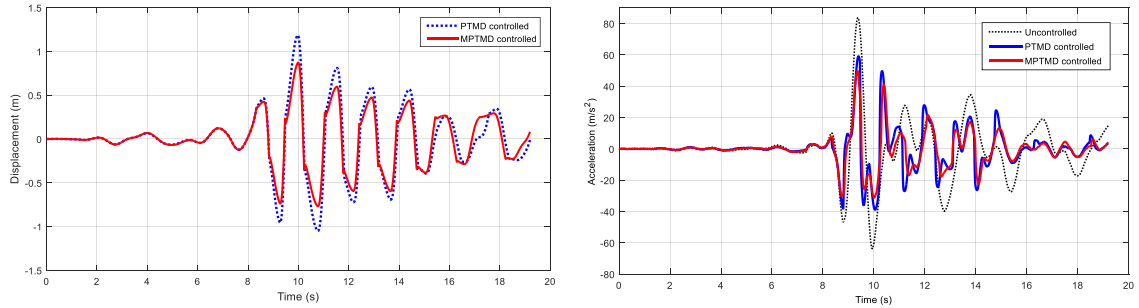


(a) 0.1 g



(b) 0.2 g

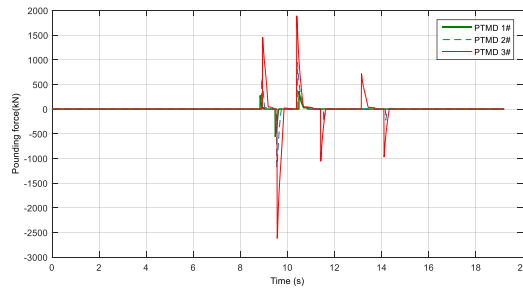
Fig. 8 Comparison of displacement and acceleration responses and pounding force on the tower top



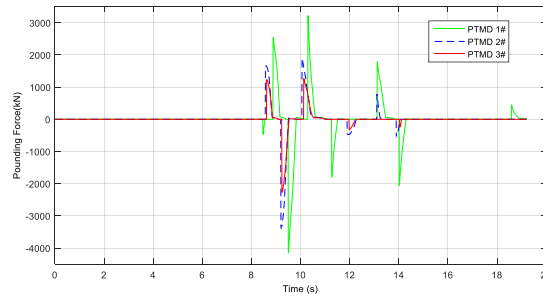
(c) 0.3 g

Fig. 8 Continued

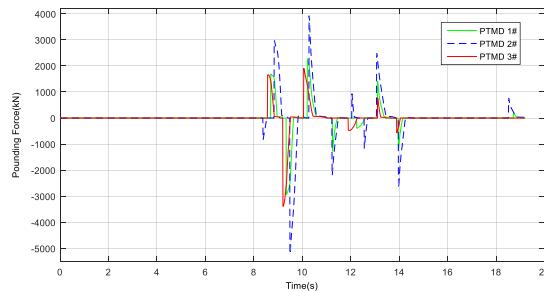
(Tianjin earthquake record, 0.1 g to 0.3 g)



(a) 0.1 g



(b) 0.2 g



(c) 0.3 g

Fig. 9 Comparison of the pounding force under Tianjin earthquake excitation (0.1 g to 0.3 g)

Table 4 Comparison of control effectiveness with the variation of excitation intensity

Excitations Responses	Peak Displacement (m)			Reduction ratio (%)		Peak Acceleration (m/s <sup>2</sup> )			Reduction ratio (%)		
	Uncontrolled	M-PTMD	PTMD	M-PTMD	PTMD	Uncontrolled	M-PTMD	PTMD	M-PTMD	PTMD	
0.1 g	x	1.512	0.413	0.521	72.9	65.6	27.886	19.643	20.313	29.6	27.2
	RMS	0.613	0.121	0.144	80.3	76.5	6.018	4.291	4.501	28.7	25.2
	y	1.115	0.338	0.422	70.3	62.2	22.175	17.37	20.257	21.7	8.7
	RMS	0.381	0.152	0.174	60.1	54.3	4.290	3.801	4.086	11.4	4.8
0.2 g	x	3.304	0.685	0.927	79.4	72.1	60.975	35.821	38.141	41.3	37.5
	RMS	1.327	0.196	0.246	85.2	81.5	13.157	7.638	8.516	41.9	35.3
	y	2.425	0.523	0.694	75.6	71.5	48.488	32.408	33.734	33.2	30.4
	RMS	0.835	0.196	0.242	76.5	71.0	9.380	8.377	8.926	10.7	4.8
0.3 g	x	4.544	0.885	1.202	80.6	73.6	83.738	47.58	53.444	43.2	36.2
	RMS	1.827	0.233	0.294	87.2	83.9	18.070	9.704	11.112	46.3	38.5
	y	3.331	0.637	0.904	81.1	73.0	66.591	41.623	45.511	37.5	31.7
	RMS	1.157	0.233	0.301	79.9	74.0	12.882	11.502	12.249	10.7	4.9

comparison, in single PTMD control cases, a PTMD with a mass of 315 t is installed on top of the main tower. The dynamic responses on the tower top under different levels of excitations are shown in Fig. 8. The pounding force of each PTMD is shown in Fig. 9.

It is obvious from the figures that the pounding forces increase with the increasing excitation levels. Table 4 further compares peak displacement and peak acceleration with different control strategies under different levels of seismic excitations. Under Tianjin earthquake excitation, better control performance can be achieved by the MPTMD control. Significant reduction is found on the peak displacement responses, the control effectiveness over uncontrolled cases can reach 72.85%, 79.36% and 80.62% under earthquake excitations with the peak accelerations of 0.1 g, 0.2 g, 0.3 g, respectively. Approximately 7% improvement over that of single PTMD controlled is observed.

## 6.5 Parameter study of MPTMD cases

### 6.5.1 Uniformly distributed and non-uniformly distributed MPTMD

Following the design procedure of MTMD, the tuned frequencies are uniformly distributed, which means the interval between the adjacent tuned frequencies is the same. However, as discussed above, the advantage of PTMD can only exert when pounding reaches certain level. As a result, to generate more impact energy, another solution is to tune each PTMD in accordance with the first few natural frequencies. As compared in Table 5, the reduction ratios for both displacement and acceleration responses are always better with the non-uniformly distributed solution. Further comparison is made when more PTMDs are considered, as shown in Fig. 10. In most cases, better reduction ratio is gained by the non-uniformly distributed MPTMD. The performance of the uniformly distributed MPTMD can be effective only when the number of PTMDs reaches certain level to target at more vibration frequencies. It is noticed that, under small excitation level, the reduction ratio of uniformly distributed MPTMD might be even decreased compared to single PTMD cases. The reasons are that (i) the uniformly distributed PTMD has

smaller mass, (ii) if the number of PTMD is too small, the coverage of the frequency bands is not wide enough for each PTMD to generate enough pounding energy. Thereby, only the non-uniformly distributed MPTMD cases will be addressed in the following study.

Table 5 Reduction ratio of uniformly distributed and non-uniformly distributed MPTMDs

Excitations	Responses	Peak Displacement (m)				Reduction ratio (%)		
		Uncontrolled	PTMD	M-PTMD (uniform)	M-PTMD (non-uniform)	PTMD	M-PTMD (uniform)	M-PTMD (non-uniform)
0.1 g	<i>x</i>	1.512	0.521	0.572	0.413	65.6	62.2	72.9
	RMS	0.613	0.144	0.164	0.121	76.5	73.2	80.3
	<i>y</i>	1.115	0.422	0.497	0.338	62.2	55.4	70.3
	RMS	0.381	0.174	0.151	0.152	54.3	60.3	60.1
0.2 g	<i>x</i>	3.304	0.927	0.985	0.685	72.1	70.2	79.4
	RMS	1.327	0.246	0.354	0.196	81.5	73.3	85.2
	<i>y</i>	2.425	0.694	0.808	0.523	71.5	66.7	75.6
	RMS	0.835	0.242	0.247	0.196	71.0	70.4	76.5
0.3 g	<i>x</i>	4.544	1.202	1.168	0.885	73.6	74.3	80.6
	RMS	1.827	0.294	0.466	0.233	83.9	74.5	87.2
	<i>y</i>	3.331	0.904	0.929	0.637	73.0	72.1	81.1
	RMS	1.157	0.301	0.332	0.233	74.0	71.3	79.9

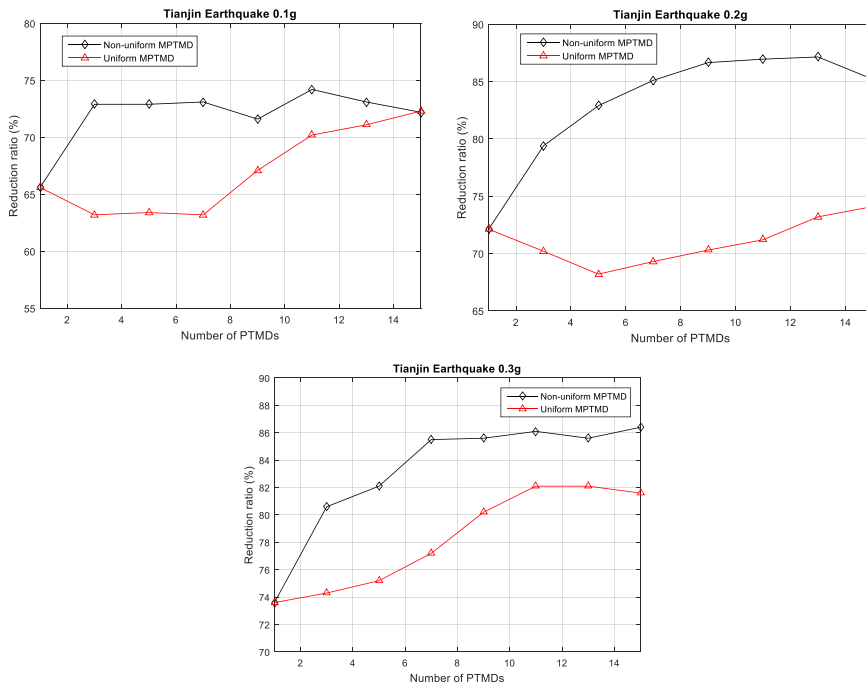


Fig. 10 Comparison of uniform MPTMD and non-uniform MPTMD

### 6.5.2 Mass ratio of MPTMD

In this section, the influence of the mass ratio on control performance is analyzed. By assuming the number of PTMD to be 3, the total mass ratio of the MPTMD is set as 0.5%, 1.0%, 1.5%, 2.0%, 2.5%, 3.0%, respectively. Each PTMD is carefully designed and tuned according to the first three natural frequencies. The gap values are decided after trial calculation to guarantee better control effectiveness. The control performance on reducing the peak displacement and acceleration of the tower top with the changing mass ratio is shown in Fig. 11. It is seen that the performance of MPTMD is better with a larger mass ratio. But the reduction ratio of acceleration varies little with the mass ratio, and increases by only 5% with the increasing mass ratio from 0.5% to 3.0%. The performance may even reduce in El Centro Earthquake excitation cases. The increase of reduction ratio on displacement control efficiency with the increasing mass ratio is obvious, while the increment becomes marginal when the mass ratio reaches certain level. Since larger mass ratio can lead to higher cost and also cause possible local damage to the main structure, a comprehensive design should be carried out to find a proper mass ratio by taking into account the control performance, the economy issue, as well as the bearing capacity of the main structure. Furthermore, it is also noticed from the figure that the optimal mass ratio is different when different excitation is selected say 0.5% under Tianjin earthquake and 0.3% under El Centro earthquake. Therefore, it is better to decide the optimal value range after the validation of more inputs.

### 6.5.3 Number of MPTMDs

As stated above, the robustness of the MPTMD control might be improved if more MPTMDs are distributed to cover wider frequency band, but too many PTMDs may be costly. For this purpose, the number of PTMD is optimized by analyzing the variation of control effectiveness with different numbers of PTMD. In the analysis, the total mass is assumed to be uniformly distributed. The gap value of each PTMD is fixed as 0.05 m. The reduction ratio is compared in Fig. 12 with different numbers of PTMD. Generally speaking, the results from the figures indicate that under Tianjin Earthquake excitation, the reduction ratio increases with the increasing number of PTMD, especially in the case of more severe earthquake excitation. The growth of the reduction

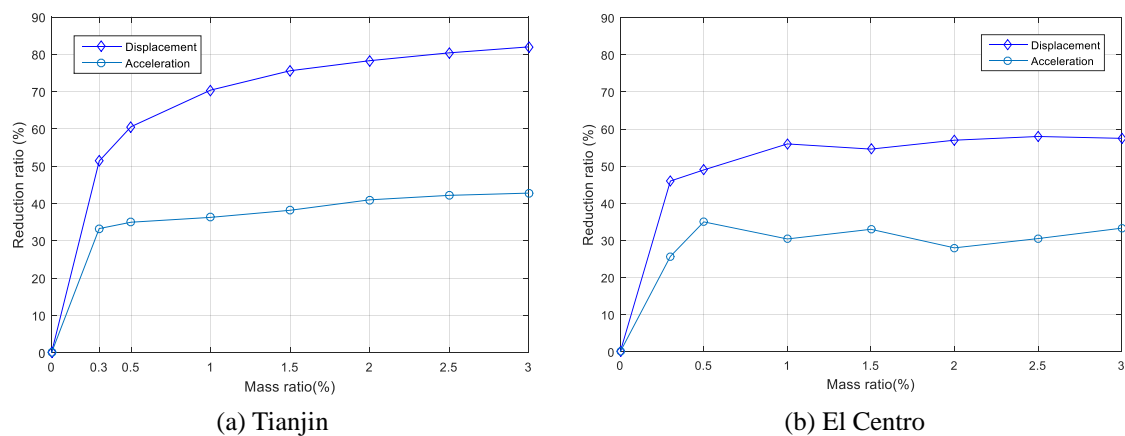


Fig. 11 Control effectiveness with different mass ratio

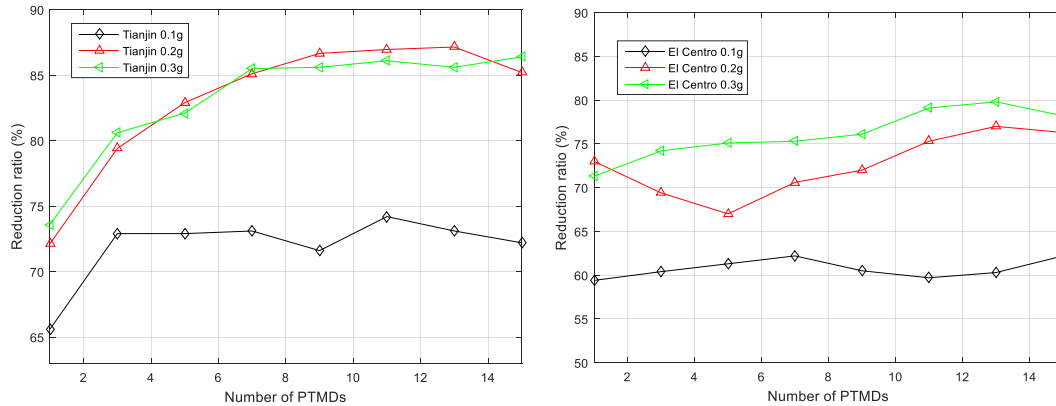


Fig. 12 Control effectiveness with different PTMD's number

ratio slows down after the total number exceeds the value of 9. Under El Centro excitation, the improvement of MPTMD control over single PTMD control is insignificant. The only improvement is found at the excitation intensity larger than 0.2 g with more than 10 PTMDs.

## 7. Conclusions

Applications of PTMD and MPTMD on controlling the responses of high-rise structures under earthquake inputs are presented in this paper. The following conclusions can be drawn:

(1) Under earthquake excitations, the PTMD has better control performance over the traditional TMD. The improvement is obvious with higher intensity level of the excitations.

(2) The control performance of the PTMD varies with the mass ratio. With the increasing mass ratio, the response reduction increases and then becomes marginal when the mass ratio reaches the optimal value. The initial gap value also affects the control effectiveness, and its optimal value varies with the frequency components of the excitation and the excitation intensity.

(3) Compared to single PTMD control, MPTMD control can further improve the reduction ratio, enhance the robustness and meanwhile reduce the mass ratio for each PTMD. Non-uniformly distributed frequencies must be considered in the design of MPTMD system.

(4) For a practical implementation, the total mass ratio of the control system can be chosen based on the desired reduction ratio and the allocated budget. And then, parameters such as gap value, numbers of PTMD should also be determined for better performance and robustness.

Based on the above analysis, it is worth mentioning that more detailed parameter study should be carried out for MPTMD control. For simplification, this paper assumed that the mass of each PTMD to be the same. Unlike TMD, the pounding force plays an important part in the control force of PTMD. Hence, the non-uniformly distributed mass for different tuned frequencies will definitely affect the energy dissipation as well as the control performance. How to decide an optimal gap value for each PTMD to guarantee a stable reduction ratio is another issue requiring further study. The optimal layout of MPTMD is an important issue to ensure the applicability of the controller. The robustness of MPTMD control should be validated when the system suffering from frequency shifts or possible errors on estimating frequencies.

## Acknowledgments

The authors are grateful for financial support by National Natural Science Foundation of China (no. 51578159 and no. 51678158), Co-operative Project in Fujian province Colleges and Universities (no. 2016H6011), and Science Project of the Education Department of Fujian Province (no. JA14057).

## References

- Alexander, N.A. and Schilder, F. (2009), "Exploring the performance of a nonlinear tuned mass damper", *J. Sound Vib.*, **319**(1), 445-462.
- Casado, C.M., Poncela, A.V. and Lorenzana, A. (2007), "Adaptive tuned mass damper for the construction of concrete piers", *Struct. Eng. Int.*, **17**(3), 252-255.
- Chung, L.L., Wu, L.Y., Huang, H.H., Chang, C.H. and Lien, K.H. (2009), "Optimal design theories of tuned mass dampers with nonlinear viscous damping", *Earthq. Eng. Eng. Vib.*, **8**(4), 547-560.
- Eason, R.P., Sun, C., Dick, A.J. and Nagarajaiah, S. (2013), "Attenuation of a linear oscillator using a nonlinear and a semi-active tuned mass damper in series", *J. Sound Vib.*, **332**(1), 154-166.
- Flores, P., Machado, M., Silva, M.T. and Martins, J.M. (2011), "On the continuous contact force models for soft materials in multibody dynamics", *Multibody Syst. Dyn.*, **25**(3), 357-375.
- Gu, M., Chen S.R. and Chang C.C. (2001), "Parametric study on multiple tuned mass dampers for buffeting control of yangpu bridge", *J. Wind Eng. Indust. Aerodyn.*, **89**(11), 987-1000.
- Hoang, N., Fujino, Y. and Warnitchai, P. (2008), "Optimal tuned mass damper for seismic applications and practical design formulas", *Eng. Struct.*, **30**(3), 707-715.
- Ikeda, Y. (2009), "Active and semi-active vibration control of buildings in Japan-practical applications and verification", *Struct. Control Hlth. Monit.*, **16**(7-8), 703-723.
- Lee, C.L., Chen, Y.T., Chung, L.L. and Wang, Y.P. (2006), "Optimal design theories and applications of tuned mass dampers", *Eng. Struct.*, **28**(1), 43-53.
- Li, J., Hao, H. and Lo, J.V. (2015), "Structural damage identification with power spectral density transmissibility: Numerical and experimental studies", *Smart Struct. Syst.*, **15**(1), 15-40.
- Li, H.N. and Ni, X.L. (2007), "Optimization of non-uniformly distributed multiple tuned mass damper", *J. Sound Vib.*, **308**(1), 80-97.
- Li, L., Song, G. and Ou, J. (2011), "Hybrid active mass damper (AMD) vibration suppression of nonlinear high-rise structure using fuzzy logic control algorithm under earthquake excitations", *Struct. Contr. Hlth. Monit.*, **18**(6), 698-709.
- Maki, D., Ishizawa, Y., Tanaka, S., Nakahara, S., Wakayama, S. and Kohiyama, M. (2015), "Vibration characteristics change of a base-isolated building with semi-active dampers before, during, and after the 2011 Great East Japan earthquake", *Earthq. Struct.*, **8**(4), 889-913.
- Matta, E. (2015), "Seismic effectiveness of tuned mass dampers in a life-cycle cost perspective", *Earthq. Struct.*, **9**(1), 73-91.
- Mishra, S.K., Gur, S. and Chakraborty, S. (2013), "An improved tuned mass damper (SMA-TMD) assisted by a shape memory alloy spring", *Smart Mater. Struct.*, **22**(9), 095016.
- Mohtasham, M., Kazem, S., Yavar, G. and Hossein, M. (2013), "Designing optimal multiple tuned mass dampers using genetic algorithms (GAs) for mitigating the seismic response of structures", *J. Vib. Contr.*, **19**(4), 605-625.
- Nagarajaiah, S. (2009), "Adaptive passive, semiactive, smart tuned mass dampers: identification and control using empirical mode decomposition, hilbert transform, and short-term fourier transform", *Struct. Contr. Hlth. Monit.*, **16**(7-8), 800-841.
- Ni, Y.Q., Xia, Y., Lin, W., Chen, W.H. and Ko, K.M. (2012), "Shm benchmark for high-rise structures: a reduced-order finite element model and field measurement data", *Smart Struct. Syst.*, **10**(4-5), 411-426.

- Occhiuzzi, A., Spizzuoco, M. and Ricciardelli, F. (2008), "Loading models and response control of footbridges excited by running pedestrians", *Struct. Contr. Hlth. Monit.*, **15**(3), 349-368.
- Richard, F. and Yoyong, A. (2015), "Designing optimum locations and properties of mtmd systems", *Procedia Eng.*, **125**, 892-898.
- Rüdinger, F. (2006), "Optimal vibration absorber with nonlinear viscous power law damping and white noise excitation", *J. Eng. Mech.*, **132**(1), 46-53.
- Rüdinger, F. (2007), "Tuned mass damper with nonlinear viscous damping", *J. Sound Vib.*, **300**(3), 932-948.
- Said, E. and Vasant, M. (2014), "Distributed multiple tuned mass dampers for wind vibration response control of high-rise building", *J. Eng.*, **2014**, 198719.
- Shan, L., Jian, F. and Jian, L. (2014), "Three-dimensional wind-induced control using mtmd based on energy balance theory", *Appl. Mech. Mater.*, **590**, 116-120.
- Spencer Jr, B.F. and Nagarajaiah, S. (2003), "State of the art of structural control", *J. Struct. Eng.*, **129**(7), 845-856.
- Sun, W.Q. and Li, Q.B. (2009), "Tmd semi-active control with shape memory alloy", *J. Harbin Inst. Technol.*, **41**, 164-168.
- Takewaki, I., Kanamori, M., Yoshitomia, S. and Tsuji, M. (2013), "New experimental system for base-isolated structures with various dampers and limit aspect ratio", *Earthq. Struct.*, **5**(4), 461-475.
- Varadarajan, N. and Nagarajaiah, S. (2004), "Wind response control of building with variable stiffness tuned mass damper using empirical mode decomposition/hilbert transform", *J. Eng. Mech.*, **130**(4), 451-458.
- Weber, B. and Feltrin, G. (2010), "Assessment of long-term behavior of tuned mass dampers by system identification", *Eng. Struct.*, **32**(11), 3670-3682.
- Yael, D. and Oren, L. (2015), "Optimality criteria based seismic design of multiple tuned-mass-dampers for the control of 3D irregular buildings", *Earthq. Struct.*, **8**(1), 77-100.
- Zhen, M., Yongbo, P. and Li, J. (2013), "Experimental and analytical studies on stochastic seismic response control of structures with MR dampers", *Earthq. Struct.*, **5**(4), 395-416.